Effect of an Orthogonal Locking Plate and Primary Plate Working Length on Construct Stiffness and Plate Strain in an *In vitro* Fracture-Gap Model

Brett Walter de Bruyn[1] Mark Glyde[1] Robert Day[2] Giselle Hosgood[1]

[1] School of Veterinary Medicine, Murdoch University, Perth, Australia
[2] Department of Medical Engineering and Physics, Royal Perth Hospital, Perth, Australia

Address for correspondence Brett Walter de Bruyn, BSc, BVMS, GradDipEd, MVetClinStud, School of Veterinary Medicine, Murdoch University, Perth, Australia (e-mail: brettdebruyn@gmail.com).

Vet Comp Orthop Traumatol 2024;37:173–180.

Abstract

Objective The aim of this study was to compare stiffness and strain of an *in vitro* fracture-gap model secured with a primary 3.5-mm locking compression plate (LCP) at three primary plate working lengths without and with an orthogonal 2.7-mm LCP.

Study Design Primary plate screw configurations modeled short working length (SWL), medium working length (MWL), and long working length (LWL) constructs. Construct stiffness with and without an orthogonal plate during nondestructive four-point bending and torsion, and plate surface strain measured during bending, was analyzed.

Results Single plate construct stiffness was significantly, incrementally, lower in four-point bending and torsion as working length was extended. Addition of an orthogonal plate resulted in significantly higher bending stiffness for SWL, MWL, and LWL ($p < 0.05$) and torsional stiffness for MWL and LWL ($p < 0.05$). Single plate construct strain was significantly, incrementally, higher as working length was extended. Addition of an orthogonal plate significantly lowered strain for SWL, MWL, and LWL constructs ($p < 0.01$).

Conclusion Orthogonal plate application resulted in higher bending and torsional construct stiffness and lower strain over the primary plate in bending in this *in vitro* model. Working length had an inverse relationship with construct stiffness in bending and torsion and a direct relationship with strain. The inverse effect of working length on construct stiffness was completely mitigated by the application of an orthogonal plate in bending and modified in torsion.

Keywords
- orthogonal plates
- working length
- construct stiffness
- plate strain
- locking plates

Introduction

Orthogonal plate application, that is, applying a second plate at 90 degrees to a primary plate, is reported for diaphyseal fracture repair in dogs and cats.[1–3] Biomechanical reports of orthogonal locking compression plate (LCP) constructs in dogs are limited to conference proceedings of a single canine cadaveric study that investigated orthogonal constructs with a primary 3.5-mm LCP and an orthogonal 2.7-mm LCP and compared stiffness to a single 3.5-mm LCP in axial compression, four-point bending, and axial torsion.[4] In cadaveric feline hemipelves, nonlocking orthogonal constructs had higher bending stiffness and greater resistance to 1-, 2-, and 5-mm gap formation under cyclic testing compared to single plate constructs.[5] Orthogonal LCP constructs have shown higher bending and torsional stiffness and lower plate strain than single plate constructs and adjacent plate constructs in human humerus and femoral models.[6–8]

received
September 11, 2023
accepted after revision
January 8, 2024
article published online
February 8, 2024

Georg Thieme Verlag KG,
Rüdigerstraße 14,
70469 Stuttgart, Germany

DOI https://doi.org/10.1055/s-0044-1779496.
ISSN 0932-0814.

The working length of a fracture secured with an LCP is the distance between the innermost screws either side of the fracture gap.[9] Working length has shown an inverse relationship to construct stiffness and a direct relationship to plate strain in *in vitro* fracture models stabilized with an LCP.[10–14] Therefore, to maximize construct stiffness and minimize plate strain, screws should be placed as close as possible to the fracture gap to minimize working length.[13] The minimum achievable working length for a comminuted fracture repaired with an LCP is dictated by fracture configuration, and a short working length may be unattainable. Augmentation of repair with an intramedullary rod or addition of an orthogonal plate can enhance stiffness of the construct when a short working length is unattainable.[3,15] The effect of extensions in working length on stiffness and plate strain can be mitigated by the application of a 40% intramedullary rod.[11,12] The effect of orthogonal LCP application on stiffness and plate strain across different primary plate working lengths has not been investigated.

Our study aimed to determine the effect of an orthogonal LCP on bending and torsional stiffness, and on primary plate strain in bending, across three different primary LCP working lengths in an *in vitro* fracture-gap model. We hypothesized that (1) orthogonal plate application would result in higher stiffness and lower plate strain for a given working length; (2) incremental extensions of primary plate working length would result in incremental reductions in stiffness and incremental increases in primary plate strain; and (3) there would be significant interaction of orthogonal plate application and working length on construct stiffness and plate strain. All research hypotheses were tested against the null hypothesis of no difference.

Materials and Methods

Bone Models

A synthetic fracture-gap model was created using two 150-mm-long Delrin tubes (Acetal Polymer; McMaster-Carr, Illinois, United States) with an outer diameter of 15.9 mm and an inner diameter of 9.5 mm, separated by a 10-mm fracture gap. The tubes were predrilled on axial midline using a numerically controlled mill with a 2.8-mm drill bit (2.8-mm Drill Bit, Quick Coupling, 165 mm; Synthes GmbH, Oberdorf, Switzerland) and, at 90 degrees to this, a 2.0-mm drill bit (2.0-mm Drill Bit, Quick Coupling, 100 mm; Synthes GmbH) as recommended by AO (AO Foundation, Davos, Switzerland) for placement of 3.5- and 2.7-mm locking screws, respectively.[16] Five 3.5-mm screw holes and six 2.7-mm screw holes were drilled in each fragment. A 4.5-mm jig-pin hole was drilled on axial midline aligned with the 3.5-mm screw holes at the ends of the Delrin for mounting into custom loading sleeves.

Construct Assembly

Constructs were assembled by a single investigator (M.G.). Delrin tubes were stabilized with a primary 12-hole 3.5-mm LCP (Vet LCP 3.5, 12-hole: Synthes GmbH) using three 28-mm bicortical locking screws (Veterinary Locking Stardrive, 3.5 mm, Self-Tapping; Synthes GmbH) per fragment. Screws were placed using a battery-powered orthopaedic drill (System 8; Stryker, Michigan, United States) with a 1.5-Nm torque limiter (Torque Limiter, 1.5 Nm, with AO/ASIF Quick Coupling; Synthes GmbH) in accordance with the AO recommendations for application of 3.5-mm LCP.[16] Plates were applied over 1-mm spacers (Tile Spacers for 1-mm Joints; Rubi, Spain) to ensure uniform plate standoff. Three different screw configurations were used in the primary plate to create short working length (SWL), medium working length (MWL), and long working length (LWL) constructs. Screw holes were numbered from the center of the plate, with the central holes designated 1 and the outermost holes designated 6. Short working length constructs had screws in holes 6, 3, and 2; MWL constructs had screws in holes 6, 4, and 3; and LWL constructs had screws in holes 6, 5, and 4, resulting in primary plate working length of two, four, and six holes, respectively (►**Fig. 1**).

Orthogonal 16-hole 2.7-mm LCP (Vet LCP 2.7, 16-hole; Synthes GmbH) were applied using two 28-mm bicortical locking screws (Veterinary Locking Stardrive, 2.7 mm, Self-Tapping; Synthes GmbH) per fragment. Screws were placed using a battery-powered orthopaedic drill using a 0.8-Nm torque limiter (Torque Limiter, 0.8 Nm, with AO/ASIF Quick Coupling; Synthes GmbH) in accordance with the AO recommendations for application of 2.7-mm LCP.[16] Plates were applied over 1-mm spacers to ensure uniform plate standoff. Orthogonal plates had screws in holes 6 and 8 using the same naming convention as the primary plates. The innermost screws in the orthogonal plate were eccentric to the innermost screws in the primary plate, relative to the fracture gap for all constructs, so construct working length was always dictated by primary plate screw configuration (►**Fig. 2**).

Constructs

Six replicates at each working length were tested without, and then with, an orthogonal plate, for a total of 36 constructs tested. This sample size was sufficient to detect an effect size of at least 1.55, with a power of 0.8 and alpha set to 0.05. The expected effect size was 3.5 based on previous investigations.[11]

Biomechanical Testing

Nondestructive four-point bending was performed on a materials testing machine (Instron 5848; Instron, Norwood, Massachusetts, United States) with a 2-kN load cell. The Delrin tubes were secured into custom loading sleeves using the predrilled 4.5-mm jig-pin hole to prevent rotation during testing. Constructs were supported on rollers with an outer span of 350 mm and loaded through rollers with an inner span of 300 mm. Each construct was preloaded until all four rollers contacted the construct, then ramp loaded for three cycles under displacement control at 10 mm/min to a peak force of 480 N, producing a peak bending moment of 6 Nm. This bending moment was within the elastic limits of the constructs based on pilot testing and previous investigations.[11] Load was applied parallel to the screw axis of the primary plate.

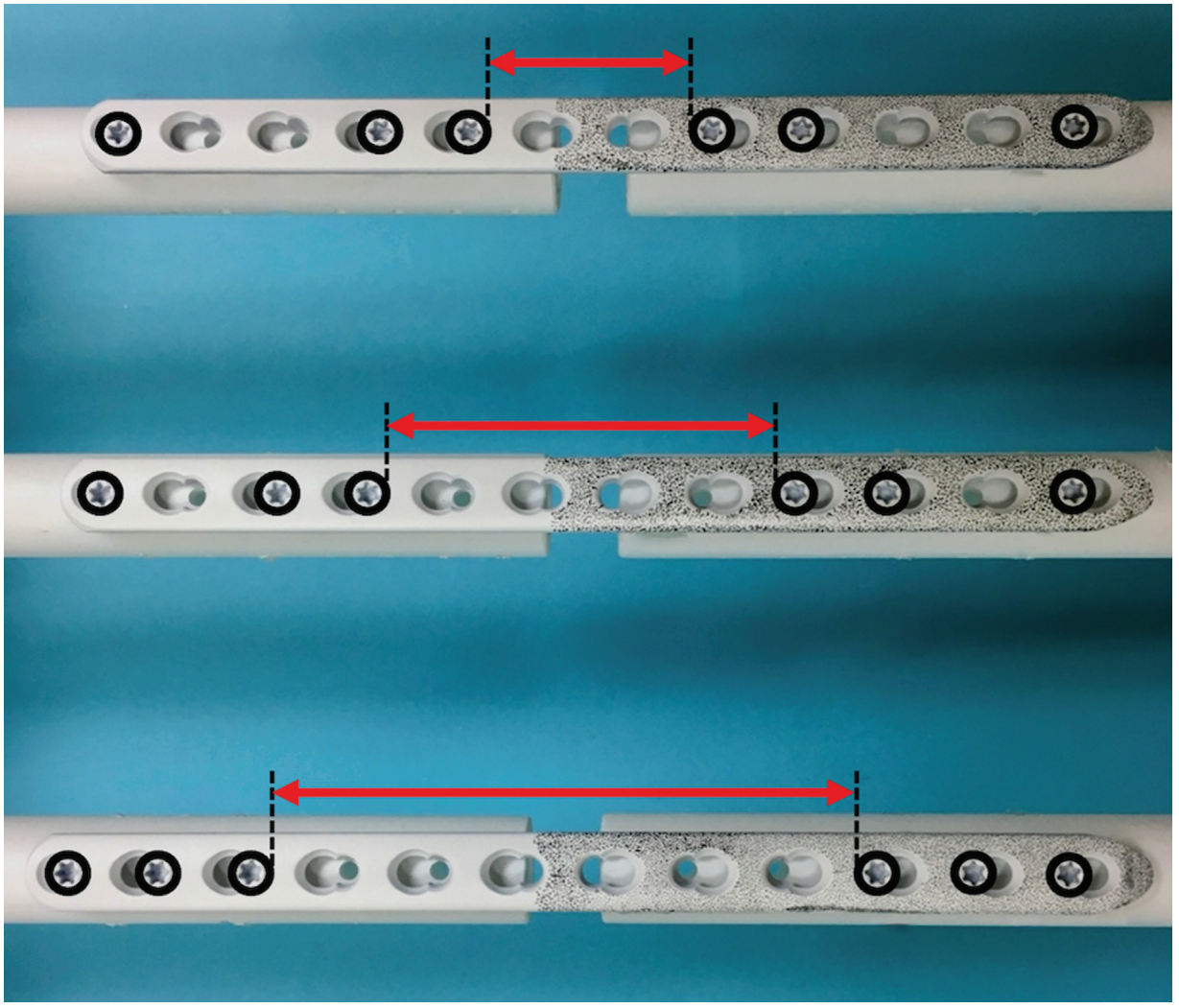

Fig. 1 Screw configuration of the primary 3.5-mm locking compression plates. Screw positions are highlighted by *hollow circles*. Short (top construct), medium (middle), and long (bottom) working lengths are indicated by the *arrows*.

Nondestructive axial torsion was performed on a materials testing machine (Instron 5566; Instron) with a 100-N load cell. The custom loading sleeve at the stacked-hole end of the construct was mounted on a secured shaft bearing allowing free rotation. A high-tensile jig screw was placed perpendicular to the materials testing machine with a moment arm of 30 mm between the rotational axis of the construct and the load arm of the testing machine. Axial load was applied to the jig screw, while the slipper-toe end of the construct was restrained, resulting in torque about the longitudinal axis of the construct. Each construct was preloaded until the load arm of the testing machine contacted the jig screw, then ramp loaded for three cycles under displacement control at 20 mm/min to a peak force of 90 N, producing a peak torque of 2.7 Nm. This torque was within the elastic limits of the constructs based on pilot testing.

Measurement of Stiffness

Stiffness data were recorded at a rate of 10 Hz. Load and actuator displacement data were examined from the third cycle for each construct as pilot testing showed that loading was consistent after the first cycle (►**Appendix 1**, available in the online version). Bending and torsional stiffness were defined as the slope of the load displacement curve and recorded as Newton per millimeter (N/mm) and Newton meter per degree (Nm/degree), respectively.

Measurement of Strain

Three-dimensional digital image correlation was used for full-field surface strain measurement in four-point bending.[10,12,14,17–22] The single plate constructs were painted matte white (White Knight Flat White; PPG Industries, New South Wales, Australia) followed by hand application of a random speckle pattern to the primary plate using a black 0.05-mm pigment ink marker pen (Pigment Liner 0.05; Staedtler, Nuernberg, Germany; ►**Fig. 3**).[14] High-definition recordings were captured during four-point bending using two high-resolution cameras with 2,448 × 2,048 pixel sensors (Grasshopper, GRAS-50S5M-C; FLIR Systems Inc, Oregon, United States). Cameras were positioned to produce a field of view spanning the fracture gap and half of the plate. Image capture was performed using VicSnap software (VicSnap; Correlated

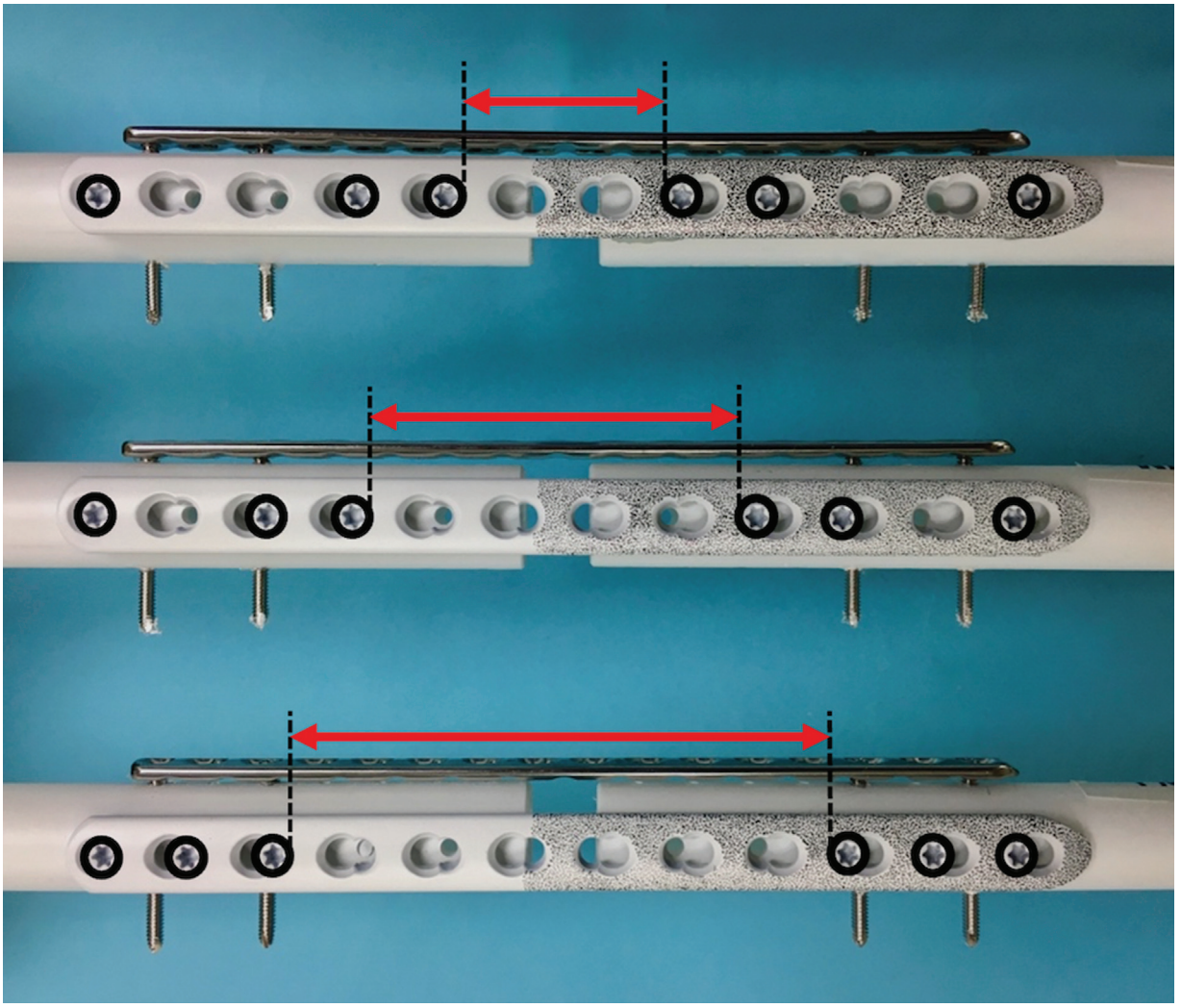

Fig. 2 Orthogonal plate constructs. Note the primary plate working lengths (indicated by the arrows) are unchanged and the orthogonal locking compression plates have constant screw position eccentric to primary plate screws.

Solutions, North Carolina, United States). This configuration resulted in speckle sizes of approximately 10 pixels, as recommended by the manufacturer.[23] Surface strain was calculated over the axial plate region between the central screw holes using Vic-3D software (Vic-3D; Correlated Solutions). The best-fitting linear model was generated from the strain versus load data for the third loading cycle of all constructs. Strain was estimated at a set force (300 N) from the linear model.

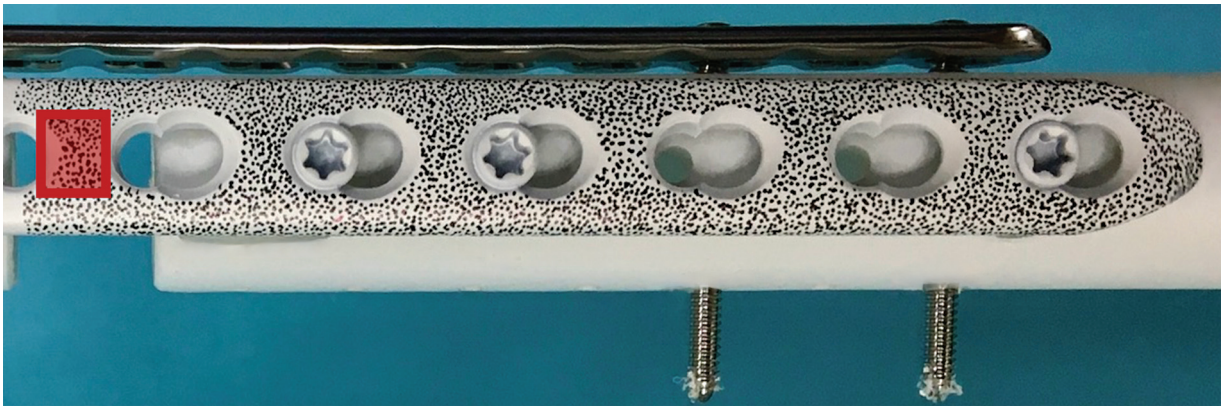

Fig. 3 Primary plate speckle pattern used for three-dimensional digital image correlation strain measurement. Strain measurement was performed at the axial plate region between the central screw holes, overlying the fracture gap (*rectangle*).

Table 1 Mean (95% confidence interval) stiffness (N/mm) in four-point bending

	Working length		
	SWL	MWL	LWL
Single plate	176.71 (171.97–181.44)[a]	154.29 (148.52–160.05)[b]	137.06 (133.84–140.28)[c]
Orthogonal	253.76 (248.60–258.92)[d]	254.01 (250.64–257.38)[d]	251.46 (250.26–252.67)[d]

Abbreviations: LWL, long working length; MWL, medium working length; SWL, short working length.
Note: Means with the same superscript letters are not significantly different ($p < 0.05$).

Table 2 Mean (95% confidence interval) stiffness (Nm/degree $\times 10^{-3}$) in axial torsion

	Working length		
	SWL	MWL	LWL
Single plate	228.47 (211.60–245.33)[a,b]	219.33 (210.29–228.36)[a]	200.69 (193.60–207.77)[c]
Orthogonal	244.55 (228.16–260.93)[b]	239.00 (232.79–245.22)[b]	225.81 (218.51–233.11)[a]

Abbreviations: LWL, long working length; MWL, medium working length; SWL, short working length.
Note: Means with the same superscript letters are not significantly different ($p < 0.05$).

Table 3 Mean (95% confidence interval) strain (mm/mm $\times 10^{-5}$) in four-point bending

	Working length		
	SWL	MWL	LWL
Single plate	235.88 (216.09–255.66)[a,d]	239.72 (222.65–256.79)[a]	267.28 (245.92–288.64)[b]
Orthogonal	189.50 (172.72-206.28)[c]	188.45 (171.29–205.61)[c]	218.77 (182.88–254.66)[d]

Abbreviations: LWL, long working length; MWL, medium working length; SWL, short working length.
Note: Means with the same superscript letters are not significantly different ($p < 0.05$).

Statistical Analysis

The responses of interest were stiffness in four-point bending (N/mm) and axial torsion (Nm/degree), and strain (mm/mm) in four-point bending. Normal distribution of responses was confirmed using the Shapiro–Wilk test and visual inspection of Q–Q plots. Responses were summarized as an estimated mean and 95% confidence interval of the mean. A two-factor, general linear model was used to assess a fixed effect of working length (i = S, M, L) and use of an orthogonal plate (j = yes, no) and its interaction on stiffness and strain. Where significant interaction was detected at $p \leq 0.05$, post hoc, planned, pairwise comparison within and across working lengths was performed against a Tukey-adjusted $p \leq 0.05$. SAS v9.4 (SAS Institute, North Carolina, United States) was used for analysis.

Results

Bending Stiffness

There was a significant interaction of working length and an orthogonal plate on stiffness in four-point bending ($p < 0.0001$; ►**Table 1**; ►**Supplementary Table S1** (available in the online version)). Pairwise comparisons across working lengths confirmed an inverse relationship of working length and stiffness, with significant incremental reduction in stiffness as working length was extended ($p < 0.05$). All constructs were significantly stiffer following the application of an orthogonal plate ($p < 0.05$) but were no longer different across primary plate working lengths.

Torsional Stiffness

There was a significant interaction of working length and an orthogonal plate on stiffness in axial torsion ($p < 0.05$; ►**Table 2**; ►**Supplementary Table S2** (available in the online version)). Pairwise comparisons across working lengths showed a reduction in stiffness from the SWL and MWL to the LWL in both the single plate and orthogonal plate constructs ($p < 0.05$). Constructs were significantly stiffer following the application of the orthogonal plate for the MWL and for the LWL ($p < 0.05$) but not for the SWL. Pairwise comparisons did not reveal a difference between the LWL orthogonal plate constructs and the SWL and MWL single plate constructs.

Strain

A significant interaction of working length and an orthogonal plate on strain in four-point bending was not detected (►**Table 3**; ►**Supplementary Table S3** (available in the online version)). Significant main effects of both working length and orthogonal plate application on plate strain were detected. Pairwise comparisons across working lengths showed an increase in strain from the SWL and MWL to the LWL in both the single plate and orthogonal plate constructs ($p < 0.05$). Constructs had significantly lower strain following

the application of an orthogonal plate for all working lengths ($p < 0.01$). Pairwise comparisons did not reveal a difference between the LWL orthogonal plate constructs and the SWL single plate constructs.

Discussion

We accepted our first research hypothesis that orthogonal plate constructs would be stiffer than single plate constructs for a given working length. This was true for all constructs in all testing modes, except SWL tested in torsion. Orthogonal plate constructs had lower strain than single plate constructs for a given working length in four-point bending.

Higher stiffness in the orthogonal plate constructs is due to greater area moment of inertia (AMI) and polar moment of inertia (PMI) compared to the single plate constructs. The AMI and PMI are the ability of an object's cross-sectional geometry to resist distortion in bending and torsion, respectively.[9,24] The AMI of a rectangular object is calculated as $AMI = \frac{(bh^3)}{12}$, where base (b) is parallel to the axis of the moment of inertia and height (h) is parallel to the direction of the applied load.[9,24] The PMI of a rectangular object is calculated as $PMI = \frac{[bh(b^2+h^2)]}{12}$. The orthogonal plate constructs act as a composite beam as the implants are firmly secured to the bone model using threaded fixation.[24] The stiffness of a composite beam is determined by the combined AMI and PMI of the implants and, in our study, were 3.7 and 1.3 times higher than the single plate constructs, respectively.[25] Our results showed correspondingly higher bending stiffness in the SWL, MWL, and LWL orthogonal plate constructs and higher torsional stiffness for both the MWL and LWL constructs. Our results are consistent with a previous canine cadaveric study that found higher bending and torsional stiffness following orthogonal plate application.[4]

Comparison within working lengths failed to detect a change in torsional stiffness following orthogonal plate application for the SWL constructs, which was unexpected. The effect size for the SWL constructs was 1.06, which is below the estimated minimum effect size of 1.55. The failure to find a difference is recorded as type II error, which could be the result of a relatively large change in AMI and a relatively small change in PMI with orthogonal plate application. Other sources of type II error such as damage to the screw–Delrin interface during torsional testing resulting in higher-than-expected variance cannot be excluded.

We selected the axial plate region between the central screw holes overlying the fracture gap for strain analysis since this was a consistent region across all working lengths that was not abutting adjacent screws. This region evaluated allowed plate strain comparison within and across working lengths under specific loading conditions and was not intended to estimate the site of peak strain. Peak strain has been reported at the narrow abaxial plate regions adjacent to screw holes overlying the fracture gap.[6,10,13,26–28] Strain mapping of the entire plate would be required to determine the peak strain location and provide information about expected regions of plate failure. This is an area of future research.

Strain was significantly lower following orthogonal plate application for all working lengths tested in four-point bending. This was expected and supports previous investigations reporting lower strain in stiffer constructs.[10,12,14,29–31] Lower strain in the orthogonal plate constructs should result in longer implant fatigue life.[32] The fatigue life of a material is inversely proportional to the stress applied with each cycle and stress is directly proportional to strain within the elastic modulus of a material.[24,33–35] Stress can therefore be computed for a specific region of interest if strain is known. Our results infer that orthogonal plate application may extend primary plate fatigue life.[32–34]

We accepted the second research hypothesis since stiffness was inversely related to working length in both bending and torsion, and strain was directly related to working length. There was a significant incremental reduction in bending stiffness as working length was extended for the single plate constructs. This is consistent with other studies where plate standoff was maintained.[10,11,13,14,28,36,37]

Strain was directly related to working length for both single and orthogonal plate constructs with LWL constructs having higher strain than SWL and MWL constructs. Our findings are consistent with previous studies documenting a direct relationship between strain and working length.[10,12–14,28,38] Studies suggest overall plate strain is distributed over a shorter segment in shorter working length constructs resulting in higher strain and this may predispose to fatigue failure.[26,27,39] Our findings, and those of others, contradict the finding of higher strain for shorter working lengths.[10,12–14,28,38]

The third research hypothesis was only accepted for results in bending and torsional stiffness where significant interaction between orthogonal plate application and working length was detected. In four-point bending, construct stiffness was no longer different across working lengths following orthogonal plate application and the inverse effect of working length on bending stiffness was completely mitigated in this model. This may be explained by creation of a composite beam and the corresponding gain in AMI achieved through orthogonal plate application.[25] In this model using the primary 3.5-mm LCP and the orthogonal 2.7-mm LCP, the orthogonal plate contributes approximately 75% of the overall AMI of the construct when tested in four-point bending. The majority contribution of the 2.7-mm LCP to overall construct AMI is likely sufficient to remove the comparatively smaller effect of change in working length on bending stiffness. In torsion, the stiffness reached in the LWL orthogonal plate constructs was no longer different to the SWL and MWL single plate constructs. This modification, rather than complete mitigation, is likely a result of the relatively smaller contribution of the orthogonal plate to the overall PMI of the construct when tested in torsion in contrast to bending.[24]

Nondestructive quasistatic four-point bending was used in this study.[10,12,28] The fatigue life of the implants was not directly assessed; however, through direct strain measurement and subsequent stress calculation, inferences can be

made regarding implant fatigue life.[32–34] We selected four-point bending to produce a constant bending moment across the entire construct during loading to allow comparison between constructs of varied stiffness. Nondestructive testing does not provide information about the yield load and ultimate strength of the constructs. Acquiring this information would provide a more complete biomechanical profile for the constructs and is an area for further investigation.

Conclusion

Application of an orthogonal 2.7-mm LCP to a primary 3.5-mm locking construct resulted in higher bending and torsional construct stiffness and lower strain over the primary plate in bending in this *in vitro* model. Longer working length constructs had lower bending and torsional stiffness and had higher strain over the primary plate in bending at the fracture gap. The inverse effect of working length on construct stiffness was mitigated by the application of an orthogonal plate in bending and modulated in torsion. These *in vitro* results may guide construct selection.

Note

An abstract of this study was presented at the Annual ECVS Congress, July 7, 2022, Porto, Portugal.

Authors' Contribution

All authors contributed to conception of the study, study design, acquisition of data, data analysis and interpretation, and manuscript preparation and review. All authors revised and approved the submitted manuscript.

Funding

This research was partially funded by a research grant from the Australian Companion Animal Health Foundation (ACAHF021). Implants used in this study were partially funded by a materials grant from Zebravet Australia.

Conflict of Interest

None declared.

References

1 Craig A, Witte PG, Moody T, Harris K, Scott HW. Management of feline tibial diaphyseal fractures using orthogonal plates performed via minimally invasive plate osteosynthesis. J Feline Med Surg 2018;20(01):6–14
2 Higuchi M, Katayama M. Clinical outcomes of orthogonal plating to treat radial and ulnar fractures in toy-breed dogs. J Small Anim Pract 2021;62(11):1001–1006
3 Brown G, Kalff S, Gemmill TJ, et al. Highly comminuted, articular fractures of the distal antebrachium managed by pancarpal arthrodesis in 8 dogs: highly comminuted, articular fractures of the canine distal antebrachium. Vet Surg 2016;45(01):44–51
4 Glyde M, Day R, Deane B. Biomechanical comparison of plate, plate-rod and orthogonal locking plate constructs in an ex-vivo canine tibial fracture gap model. Presented at: The ECVS Annual Scientific Meeting; July, 2011; Ghent, Belgium
5 Schmierer PA, Smolders LA, Zderic I, Gueorguiev B, Pozzi A, Knell SC. Biomechanical properties of plate constructs for feline ilial fracture gap stabilization. Vet Surg 2019;48(01):88–95
6 Kosmopoulos V, Nana AD. Dual plating of humeral shaft fractures: orthogonal plates biomechanically outperform side-by-side plates. Clin Orthop Relat Res 2014;472(04):1310–1317
7 El Beaino M, Morris RP, Lindsey RW, Gugala Z. Biomechanical evaluation of dual plate configurations for femoral shaft fracture fixation. BioMed Res Int 2019;2019:5958631
8 Choi JK, Gardner TR, Yoon E, Morrison TA, Macaulay WB, Geller JA. The effect of fixation technique on the stiffness of comminuted Vancouver B1 periprosthetic femur fractures. J Arthroplasty 2010;25(6, Suppl):124–128
9 Chao P, Lewis DD, Kowaleski MP, Pozzi A. Biomechanical concepts applicable to minimally invasive fracture repair in small animals. Vet Clin North Am Small Anim Pract 2012;42(05):853–872, v
10 Bird G, Glyde M, Hosgood G, Hayes A, Day R. Biomechanical comparison of a notched head locking T-plate and a straight locking compression plate in a juxta-articular fracture model. Vet Comp Orthop Traumatol 2021;34(03):161–170
11 Pearson T, Glyde M, Hosgood G, Day R. The effect of intramedullary pin size and monocortical screw configuration on locking compression plate-rod constructs in an *in vitro* fracture gap model. Vet Comp Orthop Traumatol 2015;28(02):95–103
12 Pearson T, Glyde MR, Day RE, Hosgood GL. The effect of intramedullary pin size and plate working length on plate strain in locking compression plate-rod constructs under axial load. Vet Comp Orthop Traumatol 2016;29(06):451–458
13 Stoffel K, Dieter U, Stachowiak G, Gächter A, Kuster MS. Biomechanical testing of the LCP–how can stability in locked internal fixators be controlled? Injury 2003;34(Suppl 2):B11–B19
14 Evans A, Glyde M, Day R, Hosgood G. Effect of plate–bone distance and working length on 2.0-mm locking construct stiffness and plate strain in a diaphyseal fracture gap model: a biomechanical study. Vet Comp Orthop Traumatol 2024;37(01):001–007
15 Reems MR, Beale BS, Hulse DA. Use of a plate-rod construct and principles of biological osteosynthesis for repair of diaphyseal fractures in dogs and cats: 47 cases (1994-2001). J Am Vet Med Assoc 2003;223(03):330–335
16 Johnson AL, Houlton JEF, Vannini R, eds. AO Principles of Fracture Management in the Dog and Cat. 1st ed. Vol. 148;Davos Platz, Switzerland: AO Publishing; 2005
17 Dickinson AS, Taylor AC, Browne M. The influence of acetabular cup material on pelvis cortex surface strains, measured using digital image correlation. J Biomech 2012;45(04):719–723
18 Carriero A, Abela L, Pitsillides AA, Shefelbine SJ. Ex vivo determination of bone tissue strains for an in vivo mouse tibial loading model. J Biomech 2014;47(10):2490–2497
19 Väänänen SP, Amin Yavari S, Weinans H, Zadpoor AA, Jurvelin JS, Isaksson H. Repeatability of digital image correlation for measurement of surface strains in composite long bones. J Biomech 2013;46(11):1928–1932
20 Sztefek P, Vanleene M, Olsson R, Collinson R, Pitsillides AA, Shefelbine S. Using digital image correlation to determine bone surface strains during loading and after adaptation of the mouse tibia. J Biomech 2010;43(04):599–605
21 Tiossi R, Lin L, Rodrigues RCS, et al. Digital image correlation analysis of the load transfer by implant-supported restorations. J Biomech 2011;44(06):1008–1013
22 Tiossi R, Vasco MAA, Lin L, et al. Validation of finite element models for strain analysis of implant-supported prostheses using digital image correlation. Dent Mater 2013;29(07):788–796
23 Correlated Solutions. Speckle Pattern Fundamentals Accessed September 22, 2023 at: https://correlated.kayako.com/article/38-speckle-pattern-fundamentals
24 Özkaya N, Leger D, Goldsheyder D, Nordin M. Fundamentals of Biomechanics: Equilibrium, Motion, and Deformation. Cham: Springer International Publishing; 2017
25 Gautier E, Perren SM, Cordey J. Effect of plate position relative to bending direction on the rigidity of a plate osteosynthesis. A theoretical analysis. Injury 2000;31(Suppl 3):C14–C20

26 Chen G, Schmutz B, Wullschleger M, Pearcy MJ, Schuetz MA. Computational investigations of mechanical failures of internal plate fixation. Proc Inst Mech Eng H 2010;224(01): 119–126

27 Chao CK, Chen YL, Wu JM, Lin CH, Chuang TY, Lin J. Contradictory working length effects in locked plating of the distal and middle femoral fractures-a biomechanical study. Clin Biomech (Bristol, Avon) 2020;80(07):105198–105198

28 Bird G, Glyde M, Hosgood G, Hayes A, Day R. Effect of plate type and working length on a synthetic compressed juxta-articular fracture model. VCOT Open. 2020;03(02):e119–e128

29 Kanchanomai C, Muanjan P, Phiphobmongkol V. Stiffness and endurance of a locking compression plate fixed on fractured femur. J Appl Biomech 2010;26(01):10–16

30 Matres-Lorenzo L, Diop A, Maurel N, Boucton MC, Bernard F, Bernardé A Biomechanical comparison of locking compression plate and limited contact dynamic compression plate combined with an intramedullary rod in a canine femoral fracture-gap model. Vet Surg 2016;45(03):319–326

31 Bichot S, Gibson TWG, Moens NMM, Runciman RJ, Allen DG, Monteith GM. Effect of the length of the superficial plate on bending stiffness, bending strength and strain distribution in stacked 2.0-2.7 veterinary cuttable plate constructs. An *in vitro* study. Vet Comp Orthop Traumatol 2011;24(06):426–434

32 Liu X, Zhang S, Bao Y, Zhang Z, Yue Z. Strain-controlled fatigue behavior and microevolution of 316l stainless steel under cyclic shear path. Materials (Basel) 2022;15(15):5362

33 Uematsu Y, Kakiuchi T, Hattori K, Uesugi N, Nakao F. Non-destructive evaluation of fatigue damage and fatigue crack initiation in type 316 stainless steel by positron annihilation line-shape and lifetime analyses. Fatigue Fract Eng Mater Struct 2017;40 (07):1143–1153

34 Hulse D, Hyman W, Nori M, Slater M. Reduction in plate strain by addition of an intramedullary pin. Vet Surg 1997;26(06):451–459

35 Moreno MR, Zambrano S, Dejardin LM, Saunders BW. Bone biomechanics and fracture biology. In: Johnston S, Tobias K, eds. Veterinary Surgery: Small Animal. 2nd ed. St. Louis, MO: Elsevier; 2018: 613–649

36 Bilmont A, Palierne S, Verset M, Swider P, Autefage A. Biomechanical comparison of two locking plate constructs under cyclic torsional loading in a fracture gap model. Two screws versus three screws per fragment. Vet Comp Orthop Traumatol 2015;28(05):323–330

37 Palierne S, Blondel M, Swider P, Autefage A. Biomechanical comparison of use of two screws versus three screws per fragment with locking plate constructs under cyclic loading in compression in a fracture gap model. Vet Comp Orthop Traumatol 2022;35(03):166–174

38 Wainberg SH, Moens NMM, Ouyang Z, Runciman J. The effect of working length, fracture, and screw configuration on plate strain in a 3.5-mm LCP bone model of comminuted fractures. VCOT Open. 2023;06(02):e122–e135

39 Hoffmeier KL, Hofmann GO, Mückley T. Choosing a proper working length can improve the lifespan of locked plates. A biomechanical study. Clin Biomech (Bristol, Avon) 2011;26(04):405–409